INNSPUB

Journal of Biodiversity and Environmental Sciences (JBES)
ISSN: 2220-6663 (Print) 2222-3045 (Online)
Vol. 21, No. 2, p. 148-156, 2022
http://www.innspub.net

RESEARCH PAPER OPEN ACCESS

Synthesis and characterization of chitosan with Montmorillonite nanocomposite (CNC) with enhanced antibacterial activity

T. Shanmugavadivu[1], P. Bhuvaneswari[1], G. Sabeena[2], G. Annadurai[2], E. Sindhuja[*1]

[1]*Research Department of Chemistry, Sri Paramakalyani College, Manonmaniam Sundaranar University Alwarkurichi, India*

[2]*Sri Paramakalyani Centre of Excellence in Environmental Sciences, Manonmaniam Sundaranar University, Alwarkurichi, India*

Article published on August 20, 2022

Key words: Chitosan nanoparticle, Montmorillonite, Characterization studies, Antibacterial activity

Abstract

Biopolymer chitosan nanocomposites have been synthesized using chitosan nanoparticles with the addition of montmorillonite. Here montmorillonite (MMT) acts as a nanofiller and diluted acetic acid is used as a solvent for dissolving chitosan and dispersing montmorillonite with chitosan nanoparticles. Morphology and properties of chitosan nanocomposites with and without acetic acid residue have been studied compared with those of pure chitosan. The effect of the acetic acid residue of chitosan and MMT loading in nanocomposites has been investigated. The characterization shows that the XRD Spectrum deceived that the crystallinity of the synthesized chitosan nanocomposite. FTIR spectrum revealed that the presence of elements in chitosan nanocomposites. The surface morphology of chitosan nanocomposites that were solid shaped was determined by SEM analysis, and the presence of silica and oxygen were confirmed by EDAX analysis. These prepared chitosan nanocomposites have been characterized by X-ray diffraction (XRD), Scanning electron microscopy (SEM-EDAX), Ultra Violet Spectroscopy (UV), Fourier Transform Infrared Spectroscopy (FTIR), and Particle Size Analyser (PSA). The antibacterial activity of Chitosan nanocomposite shows that the antibacterial zone of inhibition between 0.9 to 1.5mm at the concentration of 10, 20, 40, 80µl against Pseudomonas, Enterobacter, Bacillus.

***Corresponding Author:** E. Sindhuja ✉ sindhujaelangovan@gmail.com

Introduction

Nanoparticles are at the forefront of nanotechnology and have many potential applications. Nanoparticle-based methodologies in diagnostics, as well as in therapeutic areas are being developed to explore new drug targets or treatments (Kerker *et al.*, 1985; Popovtzer *et al.*, 2008). Such a wide range of applications confers risk of environmental release and human exposure. Unfortunately, information concerning the impact of nanoparticles on living organisms is just beginning to emerge (Fischer *et al.*, 2007). Numerous studies have been performed on the preparation of new organic/inorganic hybrid materials and nanocomposites (Mark *et al.*, 1996). The term "nanocomposite" is commonly used for filled polymers containing dispersed nanofillers with average particle sizes smaller than 100 nm. A variety of polymer-inorganic nanocomposites, which possess interesting electrical, optical, and magnetic properties usually superior to those of the parent polymer or inorganic species, have been reported in the works of literature (Croce *et al.*, 1998; Huyuh *et al.*, 1999; Guo *et al.*, 2000). Certain medical applications of chitin require initial insolubility accompanied by a defined biodegradability of the polymer. This is the case, for instance, for wound dressings suitable for preventing tissue adhesion in internal surgery. These materials should ideally be insoluble when positioned in the surgical wound, and undergo progressive bio-erosion leading to complete resorption, as soon as they are no longer needed. Therefore, they should be enzymatically degradable (Jolle's *et al.*, 2000). Chitosan has been widely studied for biosensors, tissue engineering, separation membrane, and water treatment, and so on, because of its good biocompatibility, biodegradability, and multiple functional groups (Kumar *et al.*, 2000).

Chitosan is a natural non-toxic biopolymer derived from the deacetylation of chitin. Chitosan and its derivatives have attracted considerable interest due to their antimicrobial and antifungal activity (Kendra *et al.*, 1984; Sudareshan *et al.*, 1992, Tsai *et al.*, 1999). Chitosan exhibits its antibacterial activity only in an acidic medium because of its poor solubility above pH (6.5) (Li *et al.*, 2002). The antibacterial activity of chitosan is influenced by several factors that include the type of chitosan, the degree of chitosan polymerization, and some of its other physicochemical properties. Chitosan nanoparticle exhibits higher antibacterial activity against Gram-positive bacteria and Gram-negative bacteria. Chitosan nanoparticles have been synthesized as a drug carrier as reported in previous studies (Janes *et al.*, 2001; De Compos *et al.*, 2001; De Compos *et al.*, 2003). Insulin-loaded chitosan nanoparticles could enhance intestinal absorption of insulin and increase its relative pharmacological bioavailability (Pan *et al.*, 2002). Chitosan nanoparticles had also been employed as a gene carrier to enhance gene transfer efficiency in cells (Mao *et al.*, 2001; Kim *et al.*, 2004). Montmorillonite clay has high cation exchange/swelling capacity, high surface area, high porosity, and better surface activity due to which it is a widely used adsorbent for the treatment of toxic organic pollutants in water purification and remediation of industrial wastes (Kim *et al.*, 1997; Meincke *et al.*, 2003; Xi *et al.*, 2004). However, the intercalation of organic surfactants between clay galleries has an effect on their surface properties, which significantly increases the basal plane spacing (Boyd *et al.*, 1988). The nanocomposites of modified clays are known to exhibit a remarkable improvement in strength/heat resistance, decrease in gas permeability/flammability, and increase in biodegradability compared to their untreated counterparts. These improvements are mainly due to the structural arrangement of organically modified clays and their interaction within the polymer matrix (Gilman *et al.*, 1999; Temuujin *et al.*, 2004).

Therefore, understanding of structural arrangements and degradation of organically modified clays is important before seeking their industrial applications. The objective of this work was to synthesize the montmorillonite clay mineral was used as model clay to explore the interactions with chitosan nanocomposites by sol-gel process. This chitosan with montmorillonite nanocomposite materials will be characterized through analytical

techniques, such as X-ray powder diffraction (XRD), Scanning electron microscopy (SEM-EDX), Ultraviolet spectroscopy (UV), Particle Size Analyser (PSA), and Fourier Transform Infrared Spectroscopy (FTIR). The antibacterial assessment was carried out using different microorganisms such as gram-positive bacteria and gram-negative bacteria.

Materials and method

Materials

All chemicals are used in this study are purely analytical grade and purchased from Merck, India, and used as obtained without additional purification. Chitosan (CS) with 80% deacetylation and Montmorillonite was purchased from Sigma-Aldrich, Acetic acid, hydrochloric acid, ethanol absolute was used as the starting materials (Sigma-Aldrich). Distilled water was used in all preparation procedures. All chemicals and reagents were of analytical grade and used without any further purification.

Preparation of Chitosan Nanoparticle

2 grams of chitosan was weighed out and dissolved in 100ml of 2 % acetic acid solution followed by continuous stirring at room temperature for about 3 hours by using a magnetic stirrer, and then 2g of sodium tripolyphosphate was dissolved in 200ml of distilled water and then added dropwise and freeze this solution in 40°C and 24hrs and then precipitate was settled at the bottom were collected and dried hot air oven 50°C at 24hrs. Finally, the prepared chitosan nanoparticle was investigated.

Preparation of chitosan with Montmorillonite Nanocomposite

Chitosan Nanocomposite was prepared in 2:2 ratios. Firstly, 2g of chitosan nanoparticle and then 2g of montmorillonite was mixed within 100ml distilled water and then this solution was shaken by using shaker for 3 days and filtered by using Whatman No: 1 filter paper. Finally, the nanocomposite was settled and then the particle was dried in a hot air oven at 24 hours and then calcinated at 500°C for 4hrs. Finally, Chitosan nanocomposite was prepared.

Antibacterial activity

Antibacterial defencelessness testing was carried out by the standard agar well diffusion method against gram-negative bacteria such as *Pseudomonas, Enterobacter,* and gram-positive bacteria such as *Bacillus subtilis* (Azam *et al.*, 2012). The bacterial cultures were grown in Nutrient broth media, for 24 h. Then, the wells were filled with a fixed volume of the Chitosan with Montmorillonite nanocomposite and water as a control. The plates were placed in a refrigerator for successive diffusion, and subsequently, the bacterial strains were incubated at 37°C for 24 h. After incubation, the diameter of the inhibition zone was determined and recorded. The experiments were performed in triplicate, and therefore, the average diameter of the inhibition zone with its standard deviation was determined.

Result and discussion

X-ray Diffraction

Fig.1 shows the XRD image of Chitosan with montmorillonite nanocomposite. XRD pattern confirms the Chitosan nanocomposite (CNC) were prepared from chitosan nanoparticles with the addition of montmorillonite as a natural reagent. XRD spectrum betrayed the crystalline of the synthesized chitosan nanocomposite (CNC) (Li *et al.*, 2020). In acidic solution it shows an extended structure that may facilitate the biopolymer intercalation in the clay interlayer space in opposition to analogous polysaccharides with coiled or helicoidal structures that are only adsorbed in the external surface of clays.

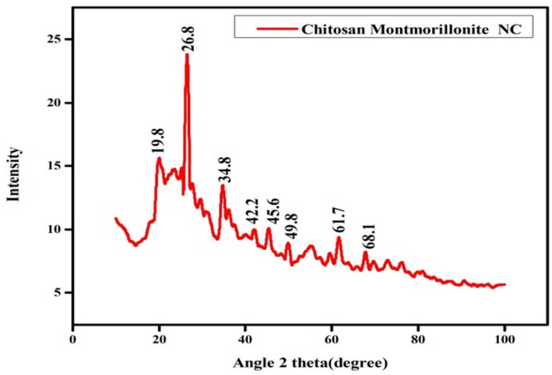

Fig. 1. XRD image of Chitosan with Montmorillonite nanocomposite.

The above graphs demonstrate eight different diffraction lattice planes for CNC. Here only one lattice plane shows more intense that is observed at the angles of 26.8 degrees respectively and other planes were 19.8, 34.8, 42.2, 45.6, 49.8, 61.7, 68.1. Similarly, some unassigned peaks were representing in this graph, it may be minerals like aluminum, magnesium, and potassium, etc. The crystallite size and crystallinity of Chitosan with montmorillonite nanocomposite was calculated according to the modified Scherrer Equation (Klug *et al.*, 1954). The average crystalline size of chitosan nanocomposite is 68nm.

Fourier Transform Infra-Red Spectroscopy

The FTIR spectrum of the chitosan nanocomposite (CNC) is shown in above Fig.2. Different IR bands were observed at 3456cm^{-1}, 2923cm^{-1}, 1100cm^{-1}, and 799cm^{-1}, respectively for CNC (Contreras-Cortes *et al.*, 2019; Pongjanyakul *et al.*, 2010). The strong band at 3456cm^{-1} represented -NH stretching of amide (II) and the band attributed to the intercalated CNC weak peak at 2923cm^{-1} indicates C-H stretching of flavonoids (Nagraha *et al.*, 2004).

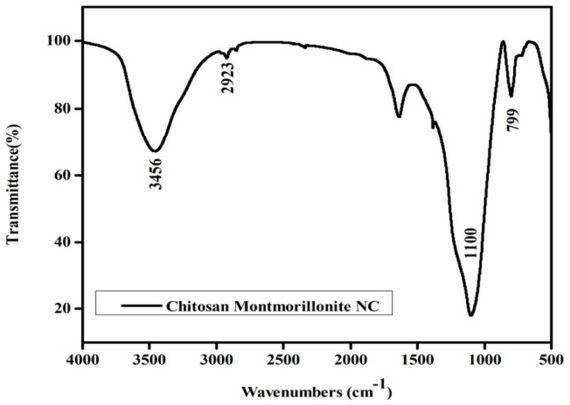

Fig. 2. FTIR image of Chitosan with Montmorillonite nanocomposite.

The band at 1100cm^{-1} was the characteristic band of C-OH stretching in secondary alcohols and the one at 799cm^{-1} could be assigned to the alkynes group of C-H bonds. The functional groups such as, C-H, -NH, C-H, and C-OH might have been derived from alkynes, amide(II), flavonoids, and secondary alcohols, which are present in the CNC. The information observed from IR spectra indicates that the molar ratio of 2:2 ratio of Chitosan nanoparticle and MMT could influence the chemical environment of the chitosan nanocomposite, and then may have an influence on absorption properties of the chitosan nanocomposites which influence to understand the binding interactions between the chitosan nanocomposite (CNC) (Sanford *et al.*, 1989; Kafshgari *et al.*, 2012).

Ultra-Violet Spectroscopy

Fig.3 represents the Ultraviolet spectroscopy of Chitosan with montmorillonite. The present study has described the synthesis of chitosan nanocomposite from chitosan nanoparticles with the addition of montmorillonite in equal molar ratios.

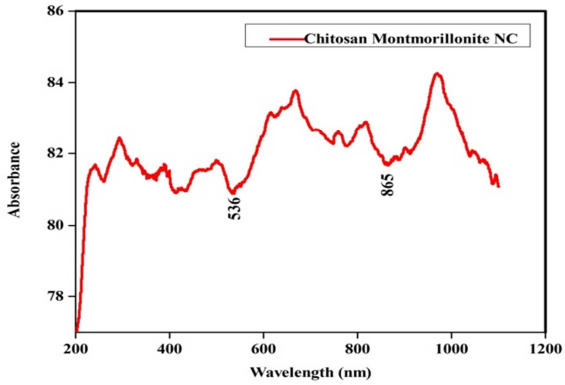

Fig. 3. UV image of Chitosan with Montmorillonite nanocomposite.

The formation of CNC in an aqueous solution was confirmed by using UV-vis spectral analysis with sharp peaks at 536nm and 865nm, respectively (Sankar *et al.*, 2014). Results showed that the generation of CNC was completed after overnight incubation at room temperature. The formation of sharp peaks at 536nm and 865nm shows the confirmation of the chitosan nanocomposite (Aziz *et al.*, 2020).

Scanning Electron Microscopy-EDAX

The SEM-EDAX image of the chitosan nanocomposite (CNC) is shown in above Fig. 4. The morphology of Chitosan nanocomposite was determined by SEM and EDAX analysis. The surface morphology of CNC using the eco-friendly method. Especially here SEM analysis shows that the sample is solid shaped (Taghizadeh *et al.*, 2020; Cui *et al.*, 2019; Wang *et al.*, 2017).

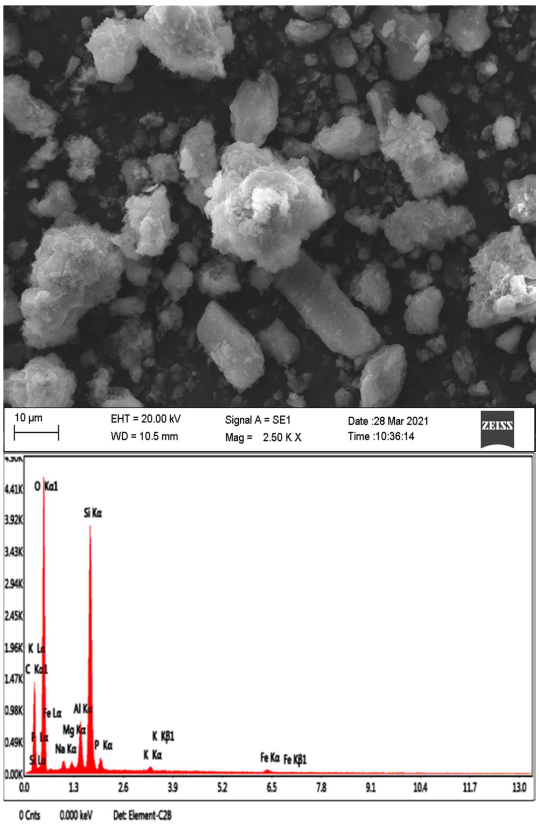

Fig. 4. SEM-EDAX image of Chitosan with Montmorillonite nanocomposite.

However, the synthesized CNC is aggregated. The average particle size of CNC is around 10 micrometers. It shows mostly solid-shaped and multiple aggregated images of CNC. EDAX revealed both qualitative and quantitative analysis of elements. The purity of synthesized CNC was found out due to the analysis of EDAX. The detective element of the CNC is C_2B. The EDAX spectrum confirms the copper elements with silica and oxygen. In this Chitosan with Montmorillonite nanocomposite, the smart quantum results revealed that the oxygen contains the highest weight percentage (89.2) and silica contains percentage (78.8). The atomic percentage is also high at oxygen (64.8) percentage and silica is (56.2) percentage. Similarly, carbon and iron were also analysed by EDAX (Singh *et al.*, 2019).

Particle Size Analyser

Particle size was determined by Dynamic Light Scattering. The average size derived from the height scan was below 100nm. A section of the XRD is included in the inset. The results from the XRD correspond to the distribution acquired from DLS (Fig. 5). The hydrodynamic diameter distribution of the Chitosan with montmorillonite nanocomposite at 68nm.

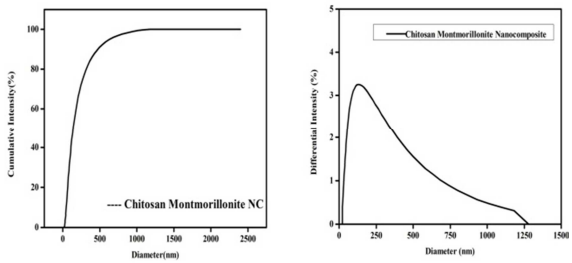

Fig. 5. PSA image of Chitosan with Montmorillonite nanocomposite.

The hydrodynamic diameter by DLS is slightly larger than that determined by XRD, as expected. The DLS and XRD analyses conducted on standard polystyrene have been compared previously and small differences between both methods and nominal values were deduced (Hoo *et al.*, 2008). A similar study has been performed elsewhere and it was observed that DLS was limited for accurate particle sizing and mostly DLS provides higher values (Baalousha *et al.*, 2012). Fig. 5 indicates that the optimized sol-gel method effectively produces a well-dispersed and narrower distribution of particle diameters. The high stability of Chitosan with montmorillonite nanocomposite is given by their very low electrostatic potential. As Chitosan with montmorillonite nanocomposite are very stable.

Antibacterial activity

The antibacterial activity of synthesized Chitosan with Montmorillonite nanocomposite has been investigated against gram-positive and gram-negative bacteria by the Agar well diffusion method (Das *et al.*, 2010; Das *et al.*, 2012; Das *et al.*, 2011; Das *et al.*, 2013).

The prepared solution with different concentrations (such as 10, 20, 40, 80µl) of Chitosan with Montmorillonite nanocomposite are placed in the broth against *Pseudomonas, Bacillus, Enterobacter* as shown in Fig. 6, respectively. The zone of inhibition on the bacterial growth has been observed as shown in Fig. 6 respectively and recorded after 24h of

incubation. The diameter of the zone has been measured using a measuring ruler. The Chitosan with Montmorillonite nanocomposite showed (Fig. 6) antibacterial activity when tested against the pathogens gram-positive and gram-negative bacteria. Table 1 shows the zone of minimum inhibition concentration which were measured in a range of 0.9 to 1.5mm in 10, 20, 40, 80µl concentration.

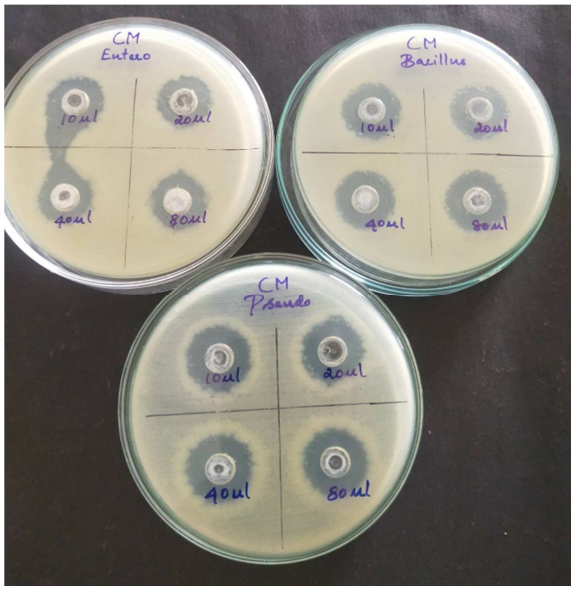

Fig. 6. Antibacterial activity image of Chitosan nanocomposite.

Table 1. Zone of inhibition of Chitosan with Montmorillonite Nanocomposite (CNC).

SN	Pathogens	CNC			
		10µl	20µl	40µl	80µl
1	*Bacillus*	1.0	1.1	1.5	1.7
2	*Enterobacter*	0.9	1.2	1.3	1.5
3	*Pseudomonas*	-	-	-	-

Conclusion

In this study Novel quaternized chitosan/ montmorillonite nanocomposite resin was successfully prepared. The resins showed a regularly spherical shape, dense structure, and good dispersibility in water. Chitosan nanoparticle with the addition of montmorillonite as a nanocomposite was succeeded through the sol-gel process. SEM analysis revealed that the Chitosan with montmorillonite nano-composite possessed a highly porous and nanostructure. Chitosan with montmorillonite nanocomposite have high stability so it is used for so many applications, this may be attributed to the good compositing between montmorillonite and Chitosan. The good properties of chitosan with montmorillonite nanocomposite may make them useful and especially for antibacterial activity because it is eco-friendly. Chitosan - montmorillonite Nanocomposite showed antibacterial activity when tested against gram-positive bacteria and gram-negative bacteria. This study shows that antibacterial activity with a high recombination rate to a suitable material willenhance its activity. Thus, chitosan-MMT nanocomposite film could be a promising novel active food packing. However, further studies are required to identify the exact antibacterial mechanism of Chitosan-MMT nanocomposite in the polymer matrix.

Acknowledgements

T Shanmugavadivu (Register No: 19221232032005) acknowledges Sri Paramakalyani College, Manonmaniam Sundaranar University, Alwarkurichi, India. Providing the support for this research work.

References

Azam A, Ahmed AS, Oves M, Khan MS, Habib SS, Memic A. 2012. Antimicrobial activity of metal oxide nanoparticles against Gram-positive and Gram-negative bacteria: a comparative study. International Journal of Nanomedicine **7,** 6003-6009,

Aziz WJ, Abid MA, Hussein EH. 2020. Biosynthesis of CuO nanoparticles and synergistic antibacterial activity using mint leaf extract. Mater. Technol **35,** 447-451.

Baalousha M, Lead JR. 2012. Rationalizing nanomaterial sizes measured by atomic force microscopy, flow field-flow fractionation, and dynamic light scattering: sample preparation, polydispersity, and particle structure. Environmental Science and Technology **46(11),** 6134-6142.

Boyd SA, Shaobai S, Lee JF, Mortland MM. 1988. Pentachlorophenol sorption by organo-clays, Clays Clay Miner **36,** 125-130.

Carlsson G, Patring J, Kreuger J, Norrgren L, Oskarsson A. 2013. Toxicity of 15 veterinary pharmaceuticals in zebrafsh (*Danio rerio*) embryos. Aquat Toxicol **126,** 30-41.

Contreras-Cortés AG, Almendariz-Tapia FJ, Gómez-Álvarez A, Burgos-Hernández, A, Luque-Alcaraz AG, RodríguezFélix F, Quevedo-López MÁ, Plascencia-Jatomea M. 2019. Toxicological assessment of cross-linked beads of chitosan-alginate and *Aspergillus australensis* biomass, with efficiency as biosorbent for copper removal. Polymers **11,** 222.

Croce F, Appetecchi GB, Persi L, Scrosati B. 1998. Nanocomposite polymer electrolytes for lithium batteries. Nature **394,** 456.

Cui CL, Gan L, Lan XY, Li J, Zhang CF, Li F, Wang CZ, Yuan CS. 2019. Development of sustainable carrier in thermosensitive hydrogel based on chitosan/alginate nanoparticles for in situ delivery system. Polym. Compos **40,** 2187-2196,

Das R, Gang S, Nath SS, Bhattacharjee R. 2012. Preparation of linoleic acid-capped silver nanocrystals and their antimicrobial effect. IET Nanobiotechnol **6,** 81-5

Das R, Gang S, Nath SS. 2011. Preparation and antibacterial activity of silver nanocrystals. J Biomater Nanobiotechnol **2,** 472-5.

Das R, Nath SS, Chakdar D, Gope G, Bhattacharjee R. 2010. Synthesis of silver nanocrystals and their optical properties. J Exp Nanosci **5,** 357-62

Das R, Saha M, Hussain SA, Nath SS. 2013. Silver nanocrystals and their antimicrobial activity on a few bacteria. Bio Nano Sci **3,** 67-72.

De Campos, Angela M, Sanchez, Alejandro, Alonso, Maria. 2001. Chitosan nanoparticles: a new vehicle for the improvement of the delivery of drugs to the ocular surface. Application to cyclosporin . J. Int. J. Pharm **224,** 159-168.

De Campos, Yongmei Du, Yumin. 2003. Effect of molecular structure of FA on protein delivery properties of FA nanoparticles. Int. J. Pharm **250,** 215- 226.

Fischer HC, Chan WC. 2007. Nanotoxicity: the growing need for in vivo study. Curr Opin Biotechnol **18(6),** 565-71. PMID: 18160274.

Gilman JW. 1999. Flammability and thermal stability studies of polymer layered-silicate (clay) nanocomposites, Appl. Clay. Sci **15,** 31-49.

Guo LS, Yang C, Yang P, Yu J, Wang W, Ge GKL, Wong. 2000. Synthesis and Characterization of Poly (vinylpyrrolidone)- Modified Zinc Oxide Nanoparticles. Chem. Mater **12(8),** 2268-2274,

Hoocm, Starostin N, West P, Mecartney ML. 2008. A comparison of atomic force microscopy (AFM) and dynamic light scattering (DLS) methods to characterize nanoparticle size distributions, Journal of Nanoparticle Research **10(1),** 89-96.

Huynh WU, Peng X, Alivisatos AP. 1999. CdSe Nanocrystal Rods/Poly (3 hexylthiophene) Composite Photovoltaic Devices Adv. Mater **11,** 923.

Janes Kevin A, Fresneau Marie P, Marazuela Ana, Fabra Angels, Alonso Maria Jose. 2001. Chitosan nanoparticles as delivery systems for doxorubicin. J. Control. Release **73,** 255-267.

Jolle's P, Muzzarelli RAA. 2000. Chitins and chitinases. Basel: Birkhauser. Chem. Mater **12,** 2268.

Kafshgari MH, Khorram M, Mansouri M, Samimi A, Osfouri S. 2012. Preparation of alginate and chitosan nanoparticles using a new reverse micellar system. Iran. Polym. J **21,** 99-107.

Kendra DF, Hadwiger LA. 1984. Characterization of the smallest chitosan oligomer that is maximally antifungal to *Fusarium solani* and elicits pisatin formation in *Pisum sativum* Exp. Mycol **8,** 276- 281,

Kerker M. 1985. The optics of colloidal silver: Something old and something new. Journal of Colloid and Interface Science **105,** 297-314.

Kim CS, Yates DM, Heanet PJ. 1997. The layered sodium silicate magadiite: an analog to smectite for benzene sorption from water, Clays Clay Miner **45,** 881-885.

Kim, Tae Hee, Park, In Kyu, Nah, Jae Woon, Choi, Yun Jaie, Cho, Chong Su. 2004. Biomaterials **25,** 3783- 3792.

Klug HP, Alexander LE. 1954. X-ray Diffraction Procedures; John Wiley and Sons Inc.: New York, NY, USA **25,** 3783- 3792.

Kumar MR. 2000. A review of chitin and chitosan applications. React Funct Polym **46,** 1.

Li X, Li S, Lu G, Wang D, Liu K, Qian X, Xue W, Meng F. 2020. Design, synthesis and biological evaluation of novel (E)-N-phenyl-4-(pyridine-acylhydrazone) benzamide derivatives as potential antitumor agents for the treatment of multiple myeloma (MM). Bioorg. Chem **103,** 104189.

Li Zhi, Zhuang, Xu Pin, Liu, Xiao Fei, Guan, Yun Lin, Yao, Kang De. 2002. Study on antibacterial *O*-carboxymethylated chitosan/cellulose blend film from LiCl/*N*, *N*-dimethylacetamide solution. Polymer **43,** 1541-1547.

Mao, Hai-Quan, Roy, Krishnendu, Troung-Le, Vu L, Janes, Kevin A, Lin, Kevin Y, Wang, Yan Thomas J, Leong, Kam WJ. 2001. Control. Release **70,** 399-421.

Mark JE. 1996. Ceriamic-Reinforced Polymers And Polymer-Modified, Polymer Engineering And Science, December **36,** 24.

Meincke O, Hoffmann B, Dietrich C, Friedrich C. 2003. Viscoelastic properties of polystyrene nanocomposites based on layered silicates, Macromol. Chem. Phys **204,** 823-830.

Nugraha E. 2004. Suyatma Alain Copinet, Lan Tighzert, and Veronique Coma. Mechanical and barrier properties of biodegradable films made from chitosan and poly (Lactic Acid) blends. Journal of Polymers and the Environment **12(1),** 823-830.

Pan, Yan Li, Ying-jian, Zhao, Hui-ying, Zheng, Jun-min, Xu, Hui, Wei, Gang Hao, Jin-song, Cui, Fu-de. 2002. Bioadhesive polysaccharide in protein delivery system: chitosan nanoparticles improve the intestinal absorption of insulin in vivo. Int. J. Pharm **249,** 139-147.

Pongjanyakul T, Rongthong T. 2010. Enhanced entrapment efficiency and modulated drug release of alginate beads loaded with drug-clay intercalated complexes as microreservoirs. Carbohydr. Polym **81,** 409-419.

Popovtzer R, Agrawal A, Kotov NA, Popovtzer A, Balter J, Carey TE, Kopelman R. 2008. Targeted gold nanoparticles enable molecular CT imaging of cancer. Nano Lett **8,** 4593- 4596.

Sanford PA. 1989. Chitosan: Commercial uses and potential applications. In: Chitin and Chitosan - sources, Chemistry, Biochemistry, Physical Properties and Applications, Elsevier: London, UK **51,** 69

Sankar R. 2014. Green synthesis of colloidal copper oxide nanoparticles using Carica papaya and its application in photocatalytic dye degradation. Spectrochim. Acta A Mol. Biomol. Spectrosc **121,** 746-750.

Singh J, Kumar V, Kim KH, Rawat M. 2019. Biogenic synthesis of copper oxide nanoparticles using plant extract and its prodigious potential for photocatalytic degradation of dyes. Environ. Res **177,** 108569.

Sudarshan NR, Hoover DG, Knorr D. 1992. Antibacterial action of chitosan Food Biotechnol **6,** 257-272.

Taghizadeh SM, Taherpoor A, Ebrahiminezhad A. 2020. Algae and microalgae mediated synthesis of iron nanoparticles and their applications. J. Adv. Med. Sci. Appl. Technol **5,** 1-11.

Temuujin J, Jadambaa Ts, Burmaa G, Erdenechimeg Sh, Amarsanaa J, MacKenzie KJD. 2004. Characterisation of acid activated montmorillonite clay from Tuulant (Mongolia), Ceram. Int **30,** 251-255.

Tsai GJ, Su WH. 1999. Antibacterial activity of shrimp chitosan against Escherichia coli. Journal of Food Protection **62(3)**, 239-243.

Wang C, Gao X, Chen Z, Chen Y, Chen H. 2017. Preparation, characterization and application of polysaccharide-based metallic nanoparticles: A review. Polymers **9,** 689.

Xi Y, Ding Z, He H, Frost RL. 2004. Structure of organoclays an X-ray diffraction and thermogravimetric analysis study, J. Colloid Interface Sci **277,** 116-120.